The FASEB Journal express article 10.1096/fj.03-0513fje. Published online Dec. 4, 2003.

Cross-talk between vascular endothelial growth factor and semaphorin-3A pathway in the regulation of normal and malignant mesothelial cell proliferation

Alfonso Catalano,*[,1] Paola Caprari,* Sabrina Rodilossi,* Piergiacomo Betta,[†] Mario Castellucci,[‡] Andrea Casazza,[§] Luca Tamagnone,[§] and Antonio Procopio*

*Department of Molecular Pathology and Innovative Therapies, Polytechnic University of Marche, Ancona; the [†]Pathology Unit, Department of Oncology, City Hospital, Alessandria; and the [‡]Institute of Normal Human Morphology, Polytechnic University of Marche, Ancona; and the [§]Institute for Cancer Research (IRCC), University of Torino, Candiolo, Italy.

[1]Corresponding author: A. Catalano, Dipartimento di Patologia Molecolare e Terapie Innovative, Università Politecnica delle Marche, Via Ranieri 6, 60131, Ancona, Italy.
E-mail: catgfp@yahoo.it

ABSTRACT

Vascular endothelial growth factor (VEGF) and semaphorin-3A (Sema-3A) play important roles in the transduction of promitotic and antimitotic signals, respectively. Here, we report that these conflicting signals are integrated via negative feedback between VEGF and Sema-3A pathways in several primary normal, but not malignant, mesothelial cells. Unlike malignant mesothelial (MM) cells, in which VEGF induces cell proliferation, normal mesothelial (NM) cell growth was repressed by VEGF. Although both cell-types expressed an overlapping set of VEGF tyrosine-kinase receptors, only in NM cells VEGF exposure entails a p38 mitogen-activated protein kinase (MAPK)-dependent increased of Sema-3A production. Inhibition of p38 MAPK (by SB202190 and SB203580) or a dominant-negative mutant of Sema-3A receptor plexin-A1 reversed the inhibitory effects of VEGF in NM cells, increasing cyclin D1 synthesis and cell growth. Conversely, sustained activation of p38 MAPK by the p38 MAPK-activating kinases MKK3 and MKK6 or transfection with Sema-3A inhibited VEGF-induced cyclin D1 up-regulation and MM cell proliferation. Therefore, these results delineate a new role of Sema-3A in VEGF function mediated by p38 MAPK and suggest that the abrogation of regulated Sema-3A expression is responsible for VEGF-driven growth of tumor cells.

Key Words: VEGF • Sema-3A • p38 MAPK • mesothelioma • mesothelium

Normal mesothelial (NM) cells form a flat epithelial-like lining of the peritoneal, pleural, and pericardial cavities that participate actively in regulating the traffic of molecules and cells between the circulation and these body compartments (1). Malignant transformation of NM cells causes a very aggressive neoplasm, namely malignant mesothelioma (MM), having fatal outcome in a large majority of cases (2). Although asbestos fibers and/or infection of Simian Virus 40 (SV40) were associated with MM (3), the molecular mechanisms of NM cell transformation remain unknown.

Recent evidence showed that MM cells stimulate their own growth in an autocrine/paracrine fashion by releasing many growth factors, including the proangiogenic vascular endothelial growth factor (VEGF) (4). We have previously shown that VEGF potently stimulates MM cell proliferation by activating its tyrosine-kinase receptors, VEGF-R1 or flt-1 and VEGF-R2 or Flk-1/KDR (5). Moreover, VEGF is the main effector of 5-lipoxygenase and SV40 large tumor-antigen action on MM cell growth (6, 7). Thus, VEGF appears to play a key role in MM biology.

VEGF acts by binding to VEGF-R1 and VEGF-R2 and activating various signal transduction molecules. These include the phosphoinositol 3-kinase (PI3-kinase), extracellular signal-regulated kinases (ERK1/2), the c-Jun mitogen-activated protein kinase (JNK), and the p38 subfamily of mitogen-activated protein kinases (MAPK) (8). Although VEGF mitotic activity is ERK1/2- and JNK-dependent (9), a negative role for p38 MAPK was suggested in the control of cell proliferation induced by VEGF (10). This is achieved by regulation of different genes, such as cdk inhibitor $p27^{kip1}$ (11), though the full identification of p38-regulated genes is incomplete. In addition, VEGF binds neuropilin-1 (Np-1) and neuropilin-2 (Np-2), which function as VEGF coreceptors increasing the ability of VEGF to activate VEGF-Rs (12). However, Nps can also function as ligand binding subunits in receptor complexes for the class III semaphorin subfamily in association with a distinct protein family, the plexins (13). Semaphorins are chemorepulsive factors that are required for guiding neuronal axons to appropriate target cells to establish a neurological synapse (14, 15); however, they are also involved in organogenesis, vascularization, angiogenesis, and cancer progression (16). Notably, the class III semaphorins Sema-3A and Sema-3F can act as a VEGF functional competitor to VEGF-driven cell responses, including migration and cell survival (17, 18).

The role of the VEGF/VEGF-Rs and Sema-3s/Nps/plexins systems in human mesothelial cells is currently unknown. Here, we demonstrate that VEGF signaling pathways in normal, but not in malignant, mesothelial cells are intimately linked to increases in p38 MAPK activity and Sema-3A production. Overcoming the inhibitory effects of p38 MAPK or Sema-3A autocrine/paracrine loop, VEGF activates cyclin D1 and induces cell growth. Our data suggest that Sema-3A is part of a negative feedback loop that serves to restrain VEGF signaling activity by limiting the amounts of spontaneous cell growth. These observations may be important in therapeutic and diagnostic approaches to MM.

METHODS

Materials

Recombinant human VEGF was purchased from R&D Systems (Minneapolis, MN). The inhibitors SB202190, SB203580, SB202474, LY294002, PD98059, cycloheximide, L-NAME, actinomycin D, and SU-1498 were all purchased from Calbiochem (La Jolla, CA). The primary antibodies for VEGF-R1 (sc-316; 1/1000), VEGF-R2 (sc-6251; 1/1000), Np-1 (sc-5307; 1/1000), Np-2 (sc-5542; 1/1000), Sema-3A (sc-1148; 1/500), cyclin D1 (sc-246; 1/500), c-Myc (9E10) (sc-40; 1/1000), and p38 MAPK antibody (sc-728; 1/1000) were obtained from Santa Cruz Biotechnology, Inc. (Santa Cruz, CA). MKK3 antibody from Cell Signaling Technology (Beverly, MA) (1/1000), and phosphospecific ATF-2 antibody (1/1000), phosphospecific p38 MAPK antibody (9211; 1/1000), and ATF-2 antibody (1/500) from New England Biolabs (Beverly, MA).

Cells

Human MM cell lines and primary NM cells were established from patients and identified morphologically and by extensive phenotypic analysis as described previously (5–7). After two weeks in culture, >99% of NM cells stained positive for calretinin. They were then expanded and used for the experiments. NM cells were used between the third and the seventh passage. All cells were maintained in RPMI-1640 supplemented with 10% heat-inactivated fetal calf serum (FCS), 1% L-glutamine, 1% penicillin-streptomycin (complete medium) (all from HyClone, Rome, Italy) at 37°C and 5% CO_2. Non-neoplastic human mesothelial cell line (Met-5A) was described previously (19).

Proliferation assay

For time-course studies, ~4×10^4 cells/ml were seeded into 24-well plates and grown to 70% confluency over 24 h. Cells were made quiescent with FCS-free medium for 12 h before experiments and then treated with 10 ng/ml VEGF. Cells were collected after 24, 48, and 72 h, stained with trypan blue and counted. For analysis of DNA synthesis, 4 h before collection, cells were pulsed with [^{3}H]-thymidine (0.5 μCi/well) in conditioned medium. Cells were then washed with PBS^{2+}, incubated with ice-cold trichloroacetic acid (5%) for 10 min, washed again with ethanol/ether (2:1) and lysed with 0.5 ml of PBS^{2+} containing 0.5% Triton, 200 mM NH_4OH, 0.1% bovine serum albumin. 3 ml of scintillation fluid were added to lysates, and radioactivity was determined for 1 min in a β-scintillation analyzer (Tri-Carb 2100TR, Packard, Mededin, CT).

SDS-PAGE and immunoblotting

Proteins (50–75 μg/lane) were separated on 8–10% SDS-polyacrylamide gels and transferred to nitrocellulose. Transfers were blocked for 2 h at room temperature with 5% nonfat milk in TBS, 0.1% Tween 20 and then incubated overnight at 4°C in the primary antibody diluted in 5% bovine serum albumin in TBS, 0.05% Tween 20. The transfers were rinsed with TBS, 0.05% Tween 20 and incubated for 1 h at room temperature in horseradish peroxidase-conjugated goat anti-rabbit or goat anti-mouse (Bio-Rad) diluted 1/5000 in 5% nonfat milk in TBS, 0.1% Tween 20. The immunoblots were developed with the Super Signal reagent (Pierce, Rockford, IL). Protein concentration was determined by standard Bradford protein assay (Bio-Rad Lab., Hercules, CA). All Western blots were reprobed with human β-actin antibody (sc-1616; 1/1000) from Santa Cruz Biotechnology to confirm equivalent loading of protein samples. To measure the phosphorylation of VEGF-R2 at different times of VEGF stimulation (10 ng/ml), cells were lysed in SDS-sample buffer containing 0.1 mM Na_3VO_4 and 1 mM PMSF. Seventy-five micrograms of cell lysate protein was Western blotted with anti-phospho-tyrosine antibody (PY20; 1/1000) from Santa Cruz Biotechnology, and the membrane was reblotted with anti-VEGF-R2 to verify equal loading of protein in each lane.

RNA extraction and semi-quantitative RT-PCR

Total RNA was extracted using the Trizol reagent (Invitrogen Life Technologies, Milan) according to the manufacturer's indications. One μg of RNA was denatured for 5 min at 65°C and then reverse-transcribed for 45 min at 55°C using AMV RT (15 U/μl) (Life Technologies) in

a 20 μl reaction. cDNA was incubated for 5 min at 95°C to inactivate the reverse transcriptase. One microliter of cDNA was used for each amplification reaction. PCR was performed with Taq DNA Polymerase, using the buffer supplied by the manufacturer (Promega, Madison, WI). Preliminary PCR (from 20 to 50 cycles) was carried out to determine the optimal number of amplification cycles for semiquantitative evaluation. β-actin primers were used for PCR reaction control and semiquantitative analysis. Oligonucleotide primers and RT-PCR conditions for Sema-3A, Sema-3B, Sema-3F, Plexin-A1, and Plexin-A2 were described previously (13, 20). Nonretrotranscribed RNA was always used as a negative control. PCR products were separated by 1–2% agarose gel electrophoresis and visualized by ethidium bromide staining.

Plasmids and transfections

Human cDNAs encoding MKK3 (sequence data available from GenBank/EMBL/DDBJ under accession no. L36719) and MKK6 (sequence data available from GenBank/EMBL/DDBJ under accession no. U39657) were generated by PCR from mesothelial cells and subcloned into pcDNA3 vector (Invitrogen). All constructs were verified by DNA sequencing. Transient transfections of cells with the different constructs were performed using LipofectAMINETM (Life Technologies), as described previously (6, 7). Briefly, 2×10^5 cells/ml were maintained for 24 h in a complete medium. Monolayers were then washed twice with serum-free RPMI and exposed for 3 h to 2 μg of each of the plasmids coding for MKK3 or MKK6 in serum-free medium. Monolayers were then washed with serum-free medium, maintained in complete medium for 24 h, washed twice with serum-free medium, and exposed to test agents for additional 24–48 h. For transfection efficiency, 1 μg of the β-galactosidase expression plasmid pcDNA3 was cotransfected with constructs. After transfection, cells were washed twice with PBS^{2-} and results normalized for transfection efficiency by determining β-galactosidase activity with the Galacto-Light PlusTM (Tropix Inc., Bedford, MA) kit according to the manufacturer's instructions.

Lentiviral-mediated transfer of plexin cDNAs

The cDNAs encoding full-size plexin-A1 or truncated-DN-plexin-A1 lacking the cytoplasmic domain (13) were subcloned into the lentiviral transfer plasmid pRRLsin.cPPT.hCMV.Wpre (kindly provided by L. Naldini, University of Torino, Candiola, Italy). Lentiviral vectors were then produced in 293T packaging cells, transiently cotransfected with a mixture of transfer, envelope, and core-packaging plasmids, as described (21). Conditioned media containing the vectors were harvested 48 h after transfection, and incubated with a fresh culture of sparse Met5A cells, in the presence of 8 μg/μl Polybrene (Sigma) for 16 h.

Statistical analysis

Results are expressed as mean ± SD. The two-sided Student's *t* test was used for statistical comparisons. A P value ≤ 0.05 was considered statistically significant.

RESULTS

Characterization of VEGF-mediated cell growth in both MM and NM cells

We screened VEGF receptors expression, activation, and sensitivity to VEGF-mediated cell growth in several NM and MM cells. As shown in Fig. 1*A*, the Met-5A mesothelial cell line, three different primary normal mesothelial cells (NM1, NM2, NM3), and three MM cell lines derived from previously untreated MM patients (MM1, MM2, MM3) constitutively express VEGF-R1, VEGF-R2, Np-1, and Np-2 at analogous levels by Western blot analysis. However, VEGF dose-dependently reduced [^{3}H]-thymidine uptake in NM1 cells (72±7% of control, at 10 ng/ml; n=3; P≤0.05), whereas it increased DNA synthesis in MM1 cells (203±4% of control, at 10 ng/ml; n=3; P≤0.05) (Fig. 1*B*, left). Consistently, VEGF (10 ng/ml) inhibited NM1 cell growth in a time-dependent fashion (70±3% of control, after 72 h; n=3; P≤0.05), but it enhanced MM1 cell number (265±12% of control, after 72 h; n=3; P≤0.05) (Fig. 1*B*, right). Moreover, there was no induction of apoptosis in both cell types as determined by cell death ELISA kit assay (data not shown). These contrasting VEGF-induced mitotic effects between normal and malignant mesothelial cells were also observed in the other MM cells and NM cells (Table 1). Since the mitogenic effects of VEGF are mediated by VEGF-R2 (8), we also studied the VEGF-induced VEGF-R2 activation. A similar time-dependent VEGF-R2 phosphorylation by VEGF was observed in both cell types (Fig. 1*C*). Thus, opposite regulation of DNA synthesis rate by VEGF in NM cells and MM cells could not be explained by a compromised activation of its receptor.

VEGF up-regulates Sema-3A expression in NM cells

We tested whether the lack of mitogenic activity of VEGF on NM cells could be explained by the activation of antagonistic signaling mechanisms, for example, those mediated by inhibitory semaphorins. We found that VEGF increased Sema-3A mRNA in NM1 cultures, with maximum stimulation after 48 h (4.6±1.2-fold; n=3; P≤0.05). In contrast, expression of Sema-3A was lower in a base form and did not significantly increase in VEGF-treated MM1 cells (Fig. 2*A*). The gene transcription inhibitor, actinomycin D (25 μg/ml), completely suppressed VEGF-induced Sema-3A mRNA in NM1 cells, whereas the protein synthesis inhibitor cycloheximide (10 μM) had no effect (Fig. 2*B*). Thus, VEGF increased Sema-3A mRNA at the transcriptional level in NM1 cells. Gene induction was specific for Sema-3A, since neither Sema-3B, Sema-3F, nor its functional receptor plexin-A1 and plexin-A2 mRNA were changed by 10 ng/ml VEGF after 48 h (data not shown). This Sema-3A up-regulation in NM1 cells was also observed at the protein levels (6.3±1.5-fold, at 10 ng/ml VEGF after 48 h; n=3; P≤0.05) (Fig. 2*C*). Accordingly, an increase in the levels of Sema-3A secreted protein was detected in NM cells and in Met-5A upon VEGF treatment, while it was not found in MM cells (Fig. 2*D*), further indicating that Sema-3A is selectively up-regulated by VEGF in NM cells.

p38 MAPK signal transduction pathways mediates VEGF-induced Sema-3A

To elucidate the VEGF signaling responsible of Sema-3A induction in NM cells, we first used pharmacological approaches. As Fig. 3*A* shows, Sema-3A up-regulation was blocked by 10 μM SU-1498, an inhibitor of VEGF-R2, suggesting an autocrine/paracrine Sema-3A stimulation by VEGF. As well, the p38 MAPK inhibitors SB202190 and SB203580 repressed VEGF-induced

Sema-3A protein expression, whereas the SB202474, an inactive structural analog of SB202190, the PI3-kinase inhibitor LY294002, the nitric oxide synthase inhibitor L-NAME, and the ERK1/2 kinase (MEK) inhibitor PD98059 were ineffective. Moreover, the effect of p38 MAPK inhibitors was dose-dependent between 0.5 and 10 μM (data not shown). Thus, p38 MAPK signaling appears the predominant pathway involved.

We then investigated how p38 MAPK was activated by VEGF in NM and MM cells. While VEGF induced only a transient activation of p38 MAPK in MM cells, it sustained a prolonged activation in NM cells. After 2 h, the mean increases in p38 MAPK phosphorylation was 4.1 ± 1.3-fold (n=3; P≤0.05) and 1.5 ± 0.6 (n=3; P=not significant) in NM1 and MM1 cells, respectively (Fig. 3*B*). At the same time, VEGF sustained the phosphorylation of one of p38 MAPK endogenous substrates, namely ATF-2, in NM1, but not in MM1 cells (Fig. 3*C*). Unlike SB202474, SB202190 treatment blocked VEGF-induced ATF-2 phosphorylation in NM1 cells, showing that this activation was p38 MAPK-dependent (Fig. 3*D*).

To confirm the regulatory role of p38 MAPK on VEGF-induced Sema-3A expression, MM1 cells were transiently cotransfected with the specific p38 MAPK kinases MKK3 and MKK6. MKK3/6 expression induced p38 MAPK activity and Sema-3A production in a VEGF-dependent manner by 3.4 ± 0.8- and 4.3 ± 1.1-fold, respectively (n=3; P≤0.05). Increases Sema-3A was fully abrogated by SB202190 (data not shown). All together, these results indicate that VEGF strongly induces p38 MAPK signaling pathway in NM cells, but not in MM cells, and that in turn this leads to enhanced Sema-3A production.

p38 MAPK activation negatively controls VEGF-induced mesothelial cell proliferation via Sema-3A-dependent pathways

We further determined the role of p38 MAPK and Sema-3A within mesothelial cells. When NM cells were preincubated with SB202190, VEGF could stimulate [^{3}H]thymidine incorporation up to 300–320%, whereas the SB202474 was ineffective (Fig. 4*A*). We observed similar results when the analogous p38 MAPK inhibitor SB203580 was used in substitution of SB202190 (data not shown). Conversely, MKK3/6 cotransfection reduced by 35–40% VEGF-induced [^{3}H]thymidine uptake in MM cells (Fig. 4*B*), which was completely rescued by SB202190 (data not shown). Thus, activated p38 MAPK exerts a negative role on both normal and malignant mesothelial cell proliferation in response to VEGF.

We next postulated that Sema-3A mediates some of these effects. Transient transfection with c-myc-tagged Sema-3A decreased by 45–50% VEGF-induced DNA synthesis in MM1 cells (Table 2), demonstrating that either p38 MAPK- and Sema-3A-dependent pathway can reduce mesothelial cell growth upon VEGF. To support the dependence on Sema-3A autocrine/paracrine loop for p38 MAPK-mediated cell proliferation, we established clones that express previously characterized wild-type plexin-A1 (WT-plexin-A1) or its dominant-negative form (DN-plexin-A1) in Met-5A cell line (Fig. 5*A*), which expressed low levels of endogenous plexin-A1 and plexin-A2 (data not shown). When DN-plexin-A1 cells were treated with VEGF, the proliferative effects were increased by 220–230% compared with WT-plexin-A1 cells or Met-5A parental cells (Table 2). In contrast, the expression of WT- or DN-plexin-A1 left unchanged VEGF-induced p38 MAPK activation (Fig. 5*B*) and Sema-3A up-regulation (Fig. 5*C*), compared with parental cells. Thus, activation of Sema-3A-dependent pathway by VEGF-

induced p38 MAPK signal is a final effector for p38 MAPK-controlled mesothelial cell proliferation.

Cyclin D1 is a target for VEGF/ Sema-3A cross-talk

Finally, we investigated what protein involved in the cell-cycle progression is the target for VEGF/Sema-3A cross-talk. Increased cyclin D1 transcription is stimulated by VEGF-induced mitotic signal (9), suggesting that Sema-3A could play a role at this level. Unlike NM1 cells, cyclin D1 protein synthesis was stimulated by VEGF almost threefold above base level in MM1 cells, and transient expression of Sema-3A-myc markedly inhibited this activation (Fig. 6*A*). As observed in NM1 cells, VEGF did not increase cyclin D1 synthesis in both Met-5A parental cells and WT-plexin-A1 engineered cells, but this was stimulated by 3.6 ± 1.2-fold (n=3; $P \leq 0.05$) in DN-plexin-A1 cells (Fig. 6*B*). Thus, events important for VEGF-induced cell-cycle progression, such as cyclin D1 up-regulation, are reduced through Sema-3A action.

DISCUSSION

Four significant findings emerge from this work. First, unlike in tumor cells, VEGF has no mitogenic activity in normal mesothelial cells, and this notwithstanding an analogous expression of VEGF receptors. Second, the absence of VEGF mitogenic signaling in normal cells parallels its capacity to increase Sema-3A production through p38 MAPK-dependent signaling. Third, Sema-3A suppresses mesothelial mitogenesis by an autocrine/paracrine mechanism, involving a plexin-dependent signaling pathway. In response to VEGF, therefore, there seems to be a limited increase of DNA synthesis, due to reduced up-regulation of cyclin D1. Fourth, activation of p38-MAPK- and Sema-3A-dependent signals partially restrains the intrinsic mitogenic activity of VEGF in tumor cells.

To our knowledge, evidence on how VEGF signaling could induce divergent responses in normal and malignant cell types have not been previously reported. Because VEGF can interact with multiple members of the VEGF receptor family, it is possible that its distinct effects depend on the specific receptor expressed by target cells. However, it is also likely that intracellular mechanisms regulate VEGF cell-specific responses. The studies aimed at elucidating the role of VEGF in tumor biology have focused primarily on the ability of VEGF to induce angiogenesis (22). Recently, we and others have shown that VEGF directly influences, by an autocrine mechanism, cell growth of several cancer cells, such as mesothelioma, melanoma, and Kaposi sarcoma (5, 23). This implies that VEGF signaling regulates a variety of processes involved in tumor progression, including cell proliferation, migration, degradation of extracellular matrix, as well as angiogenesis.

The function of VEGF/VEGF receptor system is unlikely to be restricted to malignant cells. Previous studies identified mesothelial cells as the main cellular source of VEGF in the serous cavities and indicated it as a factor that induces mesothelium fenestrations increasing the traffic of molecules and cells between the circulation and pleural/peritoneal compartments (24). We showed that the Met-5A mesothelial cell line, three different primary normal mesothelial cells, and three MM cell lines derived from previously untreated MM patients express comparable protein levels of VEGF cognate receptors. We further demonstrated that the mitogenic receptor VEGF-R2 is functional in both normal and malignant mesothelial cells, but normal mesothelial

cells show impaired viability in response to VEGF (Fig. 1 and Table 1). Expression of VEGF receptors and the absence of VEGF autocrine growth factor activity in several nonendothelial cell lines have been described previously (25). These observations suggest that only tumor cells are configured to carry a mitogenic VEGF signal to the nucleus.

We have hypothesized that during neoplastic transformation, mesothelial cells may acquire aberrant expression/activation of the downstream signaling to VEGF, which contribute to increasing metastatic potential and poor outcome. By using RT-PCR and Western blot assays, we observed that VEGF dose- and time-dependently increases the expression of a secreted class III semaphorin, namely Sema-3A, in normal, but not malignant mesothelial cells. This was achieved at the transcriptional level, since Sema-3A mRNA up-regulation was inhibited by the gene transcription inhibitor actinomycin D, but not by the protein synthesis inhibitor cycloheximide (Fig. 2). We further demonstrated that activation of VEGF-R2 receptor tyrosine-kinase and, subsequently, of p38 MAPK were required in Sema-3A up-regulation, as selective pharmacological inhibition of their tyrosine-kinase repressed VEGF-induced Sema-3A expression. p38 MAPK was strongly activated by VEGF in mesothelial cells for an extended time producing an increase of its downstream target molecules, such as ATF-2 (26), whereas only a transient activation was observed in mesothelioma cells (Fig. 3). Consistently, coexpression of a constitutively active form of MKK6 and MKK3 also increased p38 MAPK activity and, in turn, Sema-3A expression in mesothelioma cells (data not shown). Thus, p38 MAPK-dependent signaling was the dominant pathway involved in VEGF-induced Sema-3A up-regulation, though additional work will be required to definitively conclude which p38 MAPK isoform(s) are implicated.

The importance of this VEGF/Sema-3A cross-activation was demonstrated in that both p38 MAPK and Sema-3A are required to negatively control VEGF-induced mesothelial proliferation (Fig. 4 and Table 2). The role of p38 MAPK in cell-cycle control has been established recently in endothelial cells (10). Our unexpected results on different p38 MAPK activation between normal and malignant mesothelial cells, still await a mechanistic explanation. One possibility is the inactivation of upstream regulators of p38 MAPK isoforms within tumor cells (27). Alternatively, since a specific subset of integrins has been shown to mediate p38 MAPK activation (28), and integrin signaling is known to synergize with pathways activated by growth factor receptors (29), VEGF might regulate p38 MAPK by impinging on integrin-dependent signaling. Consistent with this idea, it has been shown that different histotypes of mesothelioma express distinctive sets of integrin receptors, implicating a modulation of integrin signaling during tumor progression (30).

Whatever the mechanism, the role of p38 MAPK-dependent pathway in our model is mainly to increase Sema-3A expression when activated by a potential mitogenic growth factor, such as VEGF. A regulation of Sema-3A levels following treatment with angiogenic factors, such as VEGF, had not been previously reported. Moreover, our finding that Sema-3A is an important mediator for VEGF-induced p38 MAPK to control cell proliferation was unanticipated. In fact, expression of a dominant negative mutant of Sema-3A receptor plexin-A1 left unchanged p38 MAPK activation and Sema-3A up-regulation, but unleashed the mitogenic activity of VEGF on mesothelial cells (Table 2 and Fig. 5). Our identified role of Sema-3A and the importance of VEGF/Sema-3A cross-activation are specifically seen for the stimulation of important G_1 cell-

cycle events that lead to progression to S phase (i.e., DNA synthesis), such as up-regulation of cyclin D1 (Fig. 6).

Sema-3A, which is widely distributed in many tissues and organs, was first identified as a repelling cue in growth cone guidance, during neural development (14). Moreover, Sema-3A is believed to act as morphogenic protein, but little is known about regulation and functional relevance of Sema-3A in tumor formation and progression. Sema-3A binds Np-1/plexin-A1 receptor complexes and promotes the phosphorylation of specific downstream targets, including the collapse response mediator protein (crmp), the small GTPase rac-1, LIM kinase and glycogen synthase kinase (GSK)-3 (16). Whether any of these are required for Sema-3A-dependent growth inhibition induced by VEGF remains to be seen. However, recent evidence suggests that two other secreted class III semaphorins, Sema-3B and Sema-3F, may function as tumor suppressor genes, implicated in small-cell lung cancer (31). Consistently, Sema-3A and Sema-3F have been shown to antagonize several biological effects of VEGF in both endothelial and neuronal cells, likely via its competition with a binding site on Np-1 (17, 18). In this regard, our results indicate a possible link between p38 MAPK-dependent cell-cycle control and the regulatory effects of different semaphorins. Sema-3A, being transcriptionally induced by VEGF-induced p38 MAPK-dependent pathway, may create a negative feedback loop to modulate growth promoting VEGF signaling in mesothelial cells. In contrast, the absence of this negative regulatory pathway in tumor cells could allow their uncontrolled proliferation in response to VEGF, sustaining tumor growth.

ACKNOWLEDGMENTS

This work was supported by grants from the Associazione Italiana per la Ricerca sul Cancro (AIRC) and from the Italian Ministero dell' Università e della Ricerca Scientifica (COFIN) to A. Procopio, and from the Italian Telethon Foundation (grant E.1129) to L. Tamagnone. A. Catalano is a fellow of Fondazione Italiana per la Ricerca sul Cancro (FIRC). L. Naldini is gratefully acknowledged for providing the lentiviral transfer plasmid pRRLsin.cPPT.hCMV.Wpre. We thank Pauline Jones for her assistance in preparing the manuscript.

REFERENCES

1. Bellingan, G. J., Xu, P., Cooksley, H., Cauldwell, H., Shock, A., Bottoms, S., Haslett, C., Mutsaers, S. E., and Laurent, G. J. (2002) Adhesion molecule-dependent mechanisms regulate the rate of macrophage clearance during the resolution of peritoneal inflammation. *J. Exp. Med.* **196,** 1515–1521

2. Lee, G. Y. C., Light, R. W., and Musk, A. W. (2000) Management of malignant pleural mesothelioma: A critical review. *Curr. Opin. Pulm. Med.* **6,** 267–274

3. Klein, G., Powers, A., and Croce, C. (2002) Association of SV40 with human tumors. *Oncogene* **21,** 1141–1149

4. Mossman, B. T., and Gruenert, D. C. (2002) SV40, growth factors, and mesothelioma: another piece of the puzzle. *Am. J. Respir. Cell Mol. Biol.* **26,** 167–170

5. Strizzi, L., Catalano, A., Vianale, G., Orecchia, S., Casalini, A., Tassi, G., Puntoni, R., Mutti, L., and Procopio, A. (2001) Vascular endothelial growth factor is an autocrine growth factor in human malignant mesothelioma. *J. Pathol.* **193,** 468–475

6. Romano, M., Catalano, A., Nutini, M., D'Urbano, E., Crescenzi, C., Claria, J., Libner, R., Davi, G., and Procopio, A. (2001) 5-Lipoxygenase regulates malignant mesothelial cell survival: Involvement of vascular endothelial growth factor. *FASEB J.* **15,** 2326–2336

7. Catalano, A., Romano, M., Martinotti, S., and Procopio, A. (2002) Enhanced expression of vascular endothelial growth factor (VEGF) plays a critical role in the tumor progression potential induced by simian virus 40 large T antigen. *Oncogene* **21,** 2896–2900

8. Zachary, I., and Gliki, G. (2001) Signaling transduction mechanisms mediating biological actions of the vascular endothelial growth factor family. *Cardiovasc. Res.* **49,** 568–581

9. Pedram, A., Razandi, M., and Levin, E. R. (1998) Extracellular signal-regulated protein kinase/Jun kinase cross-talk underlies vascular endothelial cell growth factor-induced endothelial cell proliferation. *J. Biol. Chem.* **273,** 26,722–26,728

10. Issbrucker, K., Marti, H. H., Hippenstiel, S., Springmann, G., Voswinckel, R., Gaumann, A., Breier, G., Drexler, H. C., Suttorp, N., and Clauss, M. (2003) p38 MAP kinase–a molecular switch between VEGF-induced angiogenesis and vascular hyperpermeability. *FASEB J.* **17,** 262–264

11. Yu, Y., and Sato, J. D. (1999) MAP kinases, phosphatidylinositol 3-kinase, and p70 S6 kinase mediate the mitogenic response of human endothelial cells to vascular endothelial growth factor. *J. Cell. Physiol.* **178,** 235–246

12. Soker, S., Miao, H. Q., Nomi, M., Takashima, S., and Klagsbrun, M. (2002) $VEGF_{165}$ mediates formation of complexes containing VEGFR-2 and neuropilin-1 that enhance $VEGF_{165}$-receptor binding. *J. Cell. Biochem.* **85,** 357–368

13. Tamagnone, L., Artigiani, S., Chen, H., He, Z., Ming, G. I., Song, H., Chedotal, A., Winberg, M. L., Goodman, C. S., Poo, M., et al. (1999) Plexins are a large family of receptors for transmembrane, secreted, and GPI-anchored semaphorins in vertebrates. *Cell* **99,** 71–80

14. Tessier-Lavigne, M., and Goodman, S. C. (1996) The molecular biology of axon guidance. *Science* **274,** 1123–1133

15. Yu, H. H., and Kolodkin, A. L. (1999) Semaphorin signaling: a little less per-plexin. *Neuron* **22,** 11–14

16. Trusolino, L., and Comoglio, P. M. (2002) Scatter-factor and semaphorin receptors: Cell signalling for invasive growth. *Nat. Rev. Cancer* **2,** 289–300

17. Nasarre, P., Constantin, B., Rouhaud, L., Harnois, T., Raymond, G., Drabkin, H. A., Bourmeyster, N., and Roche, J. (2003) Semaphorin SEMA3F and VEGF Have Opposing Effects on Cell Attachment and Spreading. *Neoplasia* **5,** 83–92

18. Bagnard, D., Vaillant, C., Khuth, S. T., Dufay, N., Lohrum, M., Puschel, A. W., Belin, M. F., Bolz, J., and Thomasset, N. (2001) Semaphorin 3A-vascular endothelial growth factor-165 balance mediates migration and apoptosis of neural progenitor cells by the recruitment of shared receptor. *J. Neurosci.* **21,** 3332–3341

19. Ke, Y., Reddel, R. R., Gerwin, B. I., Reddel, H. K., Somers, A. N., McMenamin, M. G., LaVeck, M. A., Stahel, R. A., Lechner, J. F., and Harris, C. C. (1989) Establishment of a human in vitro mesothelial cell model system for investigating mechanisms of asbestos-induced mesothelioma. *Am. J. Pathol.* **134,** 979–991

20. Maestrini, E., Tamagnone, L., Longati, P., Cremona, O., Gulisano, M., Bione, S., Tamanini, F., Neel, B.G., Toniolo, D., and Comoglio, P.M. A family of transmembrane proteins with homology to the MET-hepatocyte growth factor receptor. *Proc. Natl. Acad. Sci. USA* **93,** 674–678

21. Follenzi, A., Ailles, L. E., Bakovic, S., Geuna, M., and Naldini, L. (2000) Gene transfer by lentiviral vectors is limited by nuclear translocation and rescued by HIV-1 pol sequences. *Nat. Genet.* **25,** 217–222

22. Carmelet, P., and Jain, R. K. (2000) Angiogenesis in cancer and other disease. *Nature* **407,** 249–257

23. Masood, R., Cai, J., Zheng, T., Smith, D. L., Hinton, D. R., and Gill, P. S. (2001) Vascular endothelial growth factor (VEGF) is an autocrine growth factor for VEGF receptor-positive human tumors. *Blood* **98,** 1904–1913

24. Grove, C. S., and Lee, Y. C. (2002) Vascular endothelial growth factor: The key mediator in pleural effusion formation. *Curr. Opin. Pulm. Med.* **8,** 294–301

25. Ferrara, N., and Davis-Smyth, T. (1997) The biology of vascular endothelial growth factor. *Endocr. Rev.* **18,** 4–25

26. Ono, K., and Han, J. (2000) The p38 signal transduction pathway: activation and function. *Cell. Signal.* **12,** 1–13

27. Wang, W., Chen, J. X., Liao, R., Deng, Q., Zhou, J. J., Huang, S., and Sun, P. (2002) Sequential activation of the MEK-extracellular signal-regulated kinase and MKK3/6-p38 mitogen-activated protein kinase pathways mediates oncogenic ras-induced premature senescence. *Mol. Cell. Biol.* **22,** 3389–3403

28. Ivaska, J., Reunanen, H., Westermarck, J., Kovisto, L., Kahari, V. M., and Heino, J. (1999) Integrin alpha2beta1 mediates isoform-specific activation of p38 and upregulation of collagen gene transcription by a mechanism involving the alpha2 cytoplasmic tail. *J. Cell Biol.* **147,** 401–416

29. Clark, E. A., and Brugge, J. S. (1995) Integrins and signal transduction pathways: The road taken. *Science* **268,** 233–239

30. Giuffrida, A., Vianale, G., Di Muzio, M., Pass, H. I., Coletti, A., Birarelli, P., Procopio, A., and Modesti, A. (1999) Mofulation of integrin expression on mesotheliomas: the role of different histotypes in invasiveness. *Int. J. Oncol.* **15,** 437–442

31. Tomizawa, Y., Sekido, Y., Kondo, M., Gao, B., Yokota, J., Roche, J., Drabkin, H., Lerman, M. I., Gazdar, A. F., and Minna, J. D. (2001) Inhibition of lung cancer cell growth and induction of apoptosis after reexpression of 3p21.3 candidate tumor suppressor gene SEMA3B. *Proc. Natl. Acad. Sci. USA* **98,** 13954–13959

Received June 20, 2003; accepted Oct. 24, 2003.

Table 1

Sensitivity to VEGF-induced DNA synthesis in both normal and malignant mesothelial cells

	[^{3}H]thymidine incorporation ($cpm \times 10^3$)
NM2 cells	56.2 ± 2.4
NM2 cells + VEGF	34.5 ± 1.1 [a]
NM3 cells	51.6 ± 1.8
NM3 cells + VEGF	32.3 ± 1.4 [a]
Met-5A cells	61.1 ± 2.5
Met-5A cells + VEGF	39.7 ± 2.0 [a]
MM2 cells	150.1 ± 3.7
MM2 cells + VEGF	377.3 ± 4.0 [a]
MM3 cells	166.4 ± 4.8
MM3 cells + VEGF	388.1 ± 4.2 [a]

The mesothelial cell line Met-5A, normal (NM2 and NM3) and malignant (MM2 and MM3) mesothelial cells were synchronized for 4 h in serum-free media.Then, cells were incubated for 20 h in the absence or presence of 10 ng/mL VEGF. VEGF incubation was followed by the addition of 0.5 μCi of [^{3}H]thymidine for an additional 4 h. Cells were next washed, lysed, and counted in a β-counter. Data are the mean ± SD from 3 independent experiments, done in duplicate.

[a] $P \leq 0.05$ versus untreated cells

Table 2

Role of Sema-3A in VEGF-induced mesothelial cell proliferation

	[^{3}H]thymidine incorporation ($cpm \times 10^3$)
MM1 cells	184.6 ± 2.8
MM1 cells + VEGF	573.1 ± 4.4 [a]
MM1 cells + pcDNA3	181.2 ± 2.7
MM1 cells + Sema-3A-myc	145.5 ± 5.3 [a]
MM1 cells + VEGF + pcDNA3	560.4 ± 3.2 [a]
MM1 cells + VEGF + Sema-3A-myc	287.5 ± 3.9 [a, b]
Met-5A cells	91.1 ± 3.4
WT-plexin-A1 cells	95.2 ± 2.2
DN-plexin-A1 cells	96.7 ± 2.6
Met-5A cells + VEGF	64.5 ± 2.3 [a]
WT-plexin-A1 cells + VEGF	61.4 ± 1.8 [a]
DN-plexin-A1 cells + VEGF	144.6 ± 3.5 [a, b]

MM1 cells were transiently transfected with 2 μg of either control vector (pcDNA3) or c-myc-tagged Sema-3A construct. After 24 h, cells were synchronized for 4 h in serum-free media, and incubated in the absence or presence of 10 ng/mL VEGF. After additional 20 h, [^{3}H]-thymidine (0.5 μCi/mL) was added for 4 h to the cells. Radioactivity in cell lysates was determined in a β-scintillation analyzer. Data represent mean ± SD from n = 3 with duplicate determinations.

[a] $P \leq 0.05$ versus MM1 cells, Met-5A cells, WT-plexin-A1 cells, or DN-plexin-A1 cells

[b] $P \leq 0.05$ versus MM1 cells plus VEGF, or Met-5A cells plus VEGF

Fig. 1

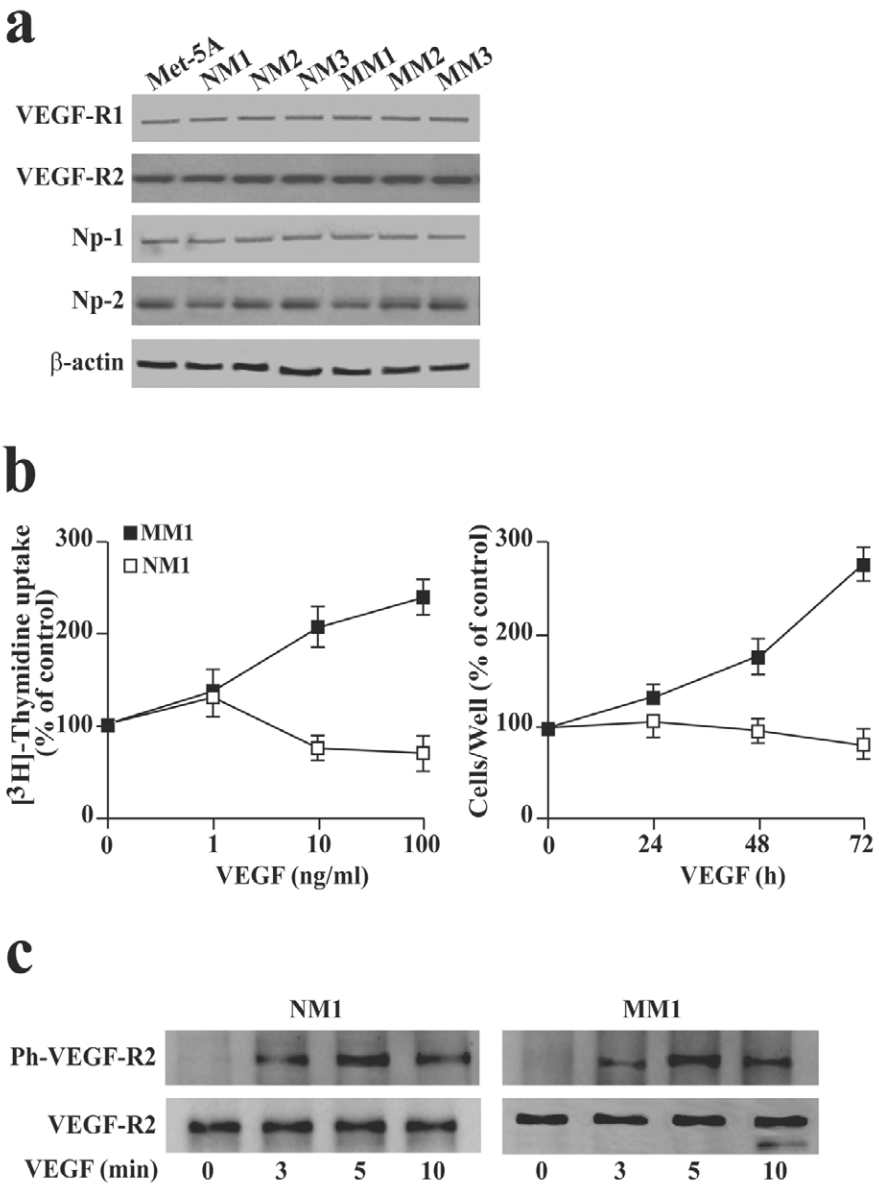

Figure 1. Expression of VEGF receptors, susceptibility to VEGF-mediated cell growth and VEGF-R2 phosphorylation in both MM and NM cells. (***a***) Cellular protein extracts (75 μg) from Met-5A mesothelial cell line, three different primary normal mesothelial cells (NM1, NM2, NM3), and three MM cell lines derived from previously untreated MM patients (MM1, MM2, MM3) were collected, separated by 8% SDS PAGE and transferred to Immobilon-P membranes (Millipore, Bedford, MA). VEGF-R1, VEGF-R2, Np-1 and Np-2 protein levels were then analyzed by Western blotting. β-actin was used as an internal control. (***b***) NM1 and MM1 cells (4×10^4/mL) were starved in serum-free culture medium for 4 h, and the cells were exposed to the indicated concentrations of VEGF for the next 24 h. Four hours before collection, cells were pulsed with [^{3}H]-thymidine (0.5 μCi/mL). Radioactivity in cell lysates was determined in a β-scintillation analyzer (table on the left). NM1 and MM1 cells (10^4/mL) were incubated with 10 ng/mL of VEGF for indicated times. Cell numbers (see table on the right) were assessed using the technique described in "Methods". Results represent the mean ± SD from 3 independent experiments and are expressed as a percentage of the control. (***C***) NM1 and MM1 were incubated with VEGF (10 ng/mL) for different times. Cellular proteins were lysed in an extraction buffer, separated by 8% PAGE and Western blotted. The filters were probed with PY20 anti-phospho-tyrosine antibody (top); then the membrane was stripped and reblotted with an anti-VEGF-R2 antibody (bottom). Data are representative from 3 independent experiments (***a*** and ***c***).

Fig. 2

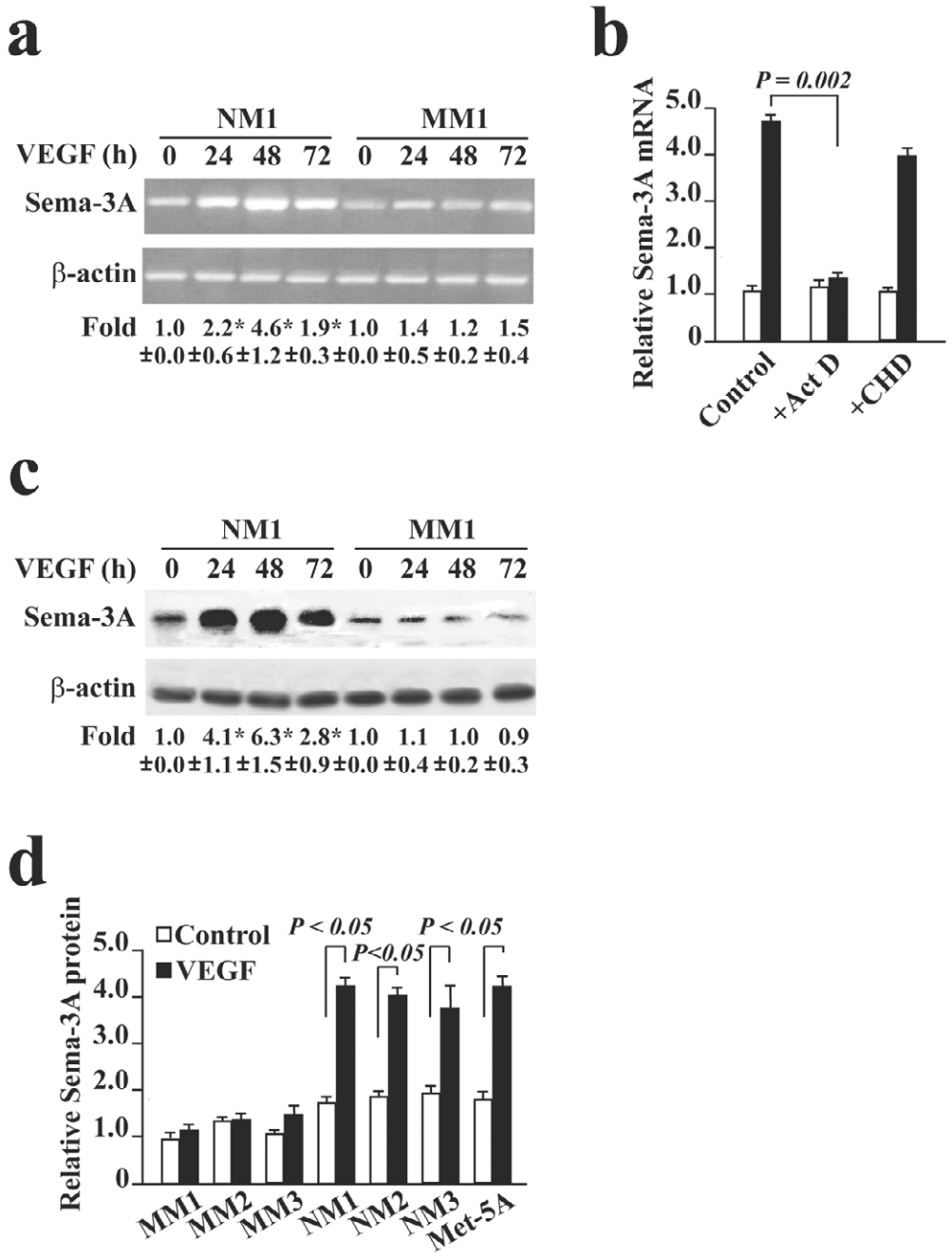

Figure 2. Sema-3A induction upon VEGF stimulation. NM1 and MM1 cells (2×10^5/mL) were exposed for different times to 10 ng/mL of VEGF (***a*** and ***c***). (***a***) Total RNA was isolated and (1 μg) subjected to RT-PCR using specific primers for Sema-3A. Amplification fragments (~300 bp) were visualized by 2% agarose gel electrophoresis and ethidium bromide staining. β-actin was used as an internal PCR control. (***b***) Relative abundance of Sema-3A mRNA analyzed by RT-PCR after 48 h in VEGF-untreated (□) and -treated (■) cells in the presence of vehicle (control), actinomycin D (Act D, 25 μg/mL), or cycloheximide (CHX, 10 μM), measured by scanning densitometry and normalized with respect to β-actin mRNA. Data represent the mean ± SD from 3 independent experiments with *P* value reported. (***c***) Cellular proteins of NM1 and MM1 were separated by SDS-PAGE and then immunoblotted with anti-Sema-3A antibody and normalized with respect to β-actin protein. Representative experiments of n=3 are shown. "Fold" indicates the relative ratio between Sema-3A and β-actin levels, determined by densitometric analysis. The relative ratio measured at time "0" is arbitrarily presented as 1. Numbers represent the mean ± SD from 3 experiments. *, $P < 0.05$ vs. time 0 (***a*** and ***c***). (***d***) Intensity of Sema-3A protein signal during VEGF exposure in NM cells, Met-5A cell line and MM cells, measured by scanning densitometry and normalized with respect to β-actin. Values are mean ± SD (n=3). The *P* value is also indicated.

Fig. 3

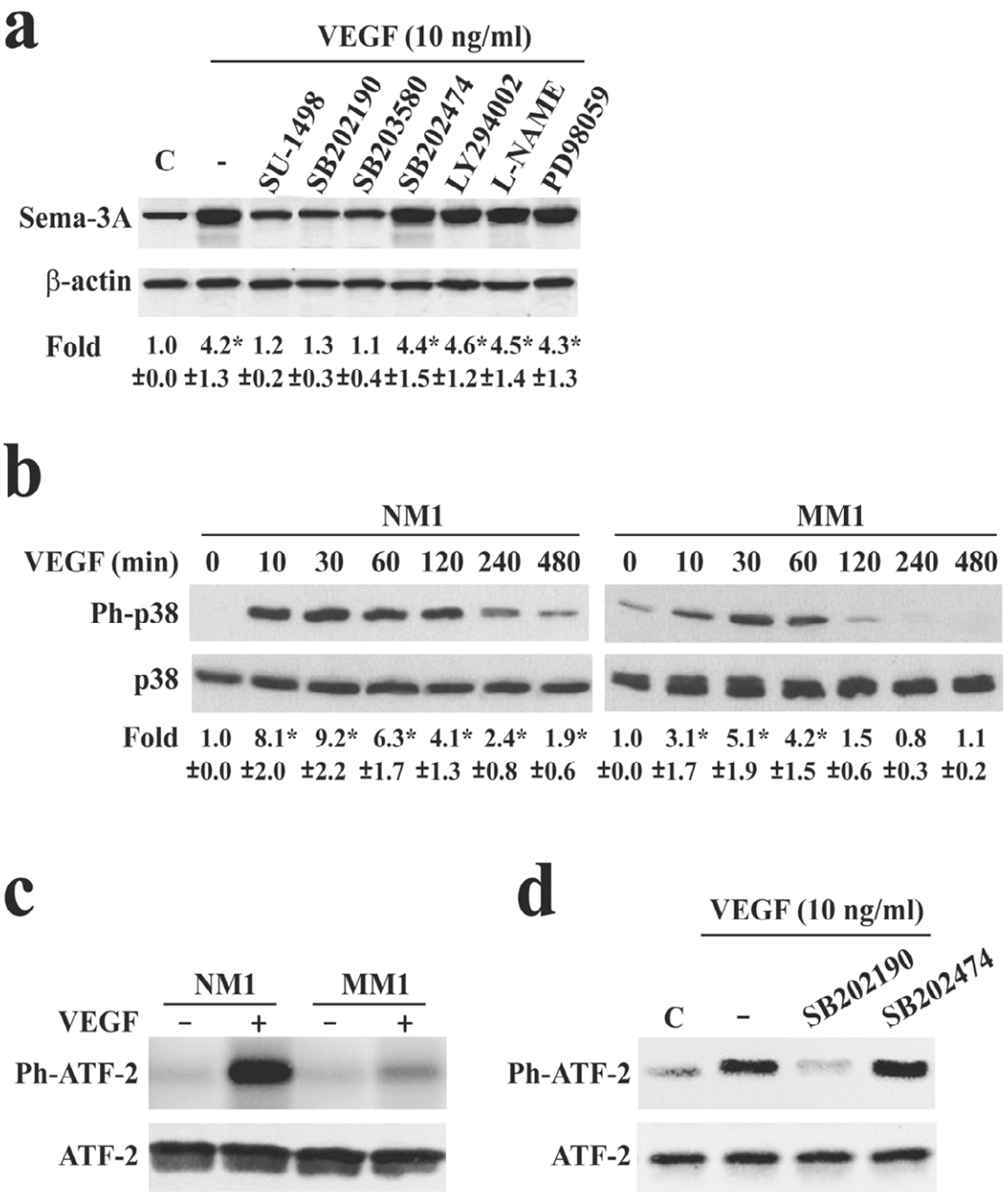

Figure 3. A p38-MAPK-dependent pathway is required for VEGF-induced Sema-3A up-regulation. (***a***) NM1 cells were treated for 2 days with VEGF (10 ng/mL) in combination with SU-1498 (10 μM), SB202190 (10 μM), SB203580 (10 μM), SB202474 (10 μM), LY294002 (10 μM), L-NAME (1 mM), or PD98059 (10 μM). Cellular proteins were then extracted and immunoblotted with anti-Sema-3A and anti-β-actin antibody. (***b***) NM1 and MM1 cells were left untreated (time "0") or treated with 10 ng/mL VEGF for 10 min to 8 h, cell extracts were prepared, and equal amounts of protein were analyzed by SDS-PAGE and immunoblotting with antibodies directed to the activated form of p38 MAPK (phospho-Thr^{180}/Tyr^{182}; top), and to total p38 MAPK (bottom). (***c***) Phosphorylation of endogenous ATF-2 was measured in protein lysates of NM1 and MM1 cells after 2 h stimulation, by Western blotting with phospho-ATF-2 (Thr^{71}) and total ATF-2 antibody. (***d***) NM1 cells were untreated or treated with SB202190 or SB202474 (10 μM), followed by treatment with 10 ng/mL VEGF. After 2 h, cellular extracts were analyzed by Western blot as described in **Fig. 3*c***. Representative data (n=3) are shown. Folds are indicated as reported in **Fig. 2**. The relative ratio measured in the control or at time "0" is arbitrarily presented as 1. Numbers represent the mean ± SD from 3 experiments. *, $P < 0.05$ vs. control or time 0 (***a*** and ***b***).

Fig. 4

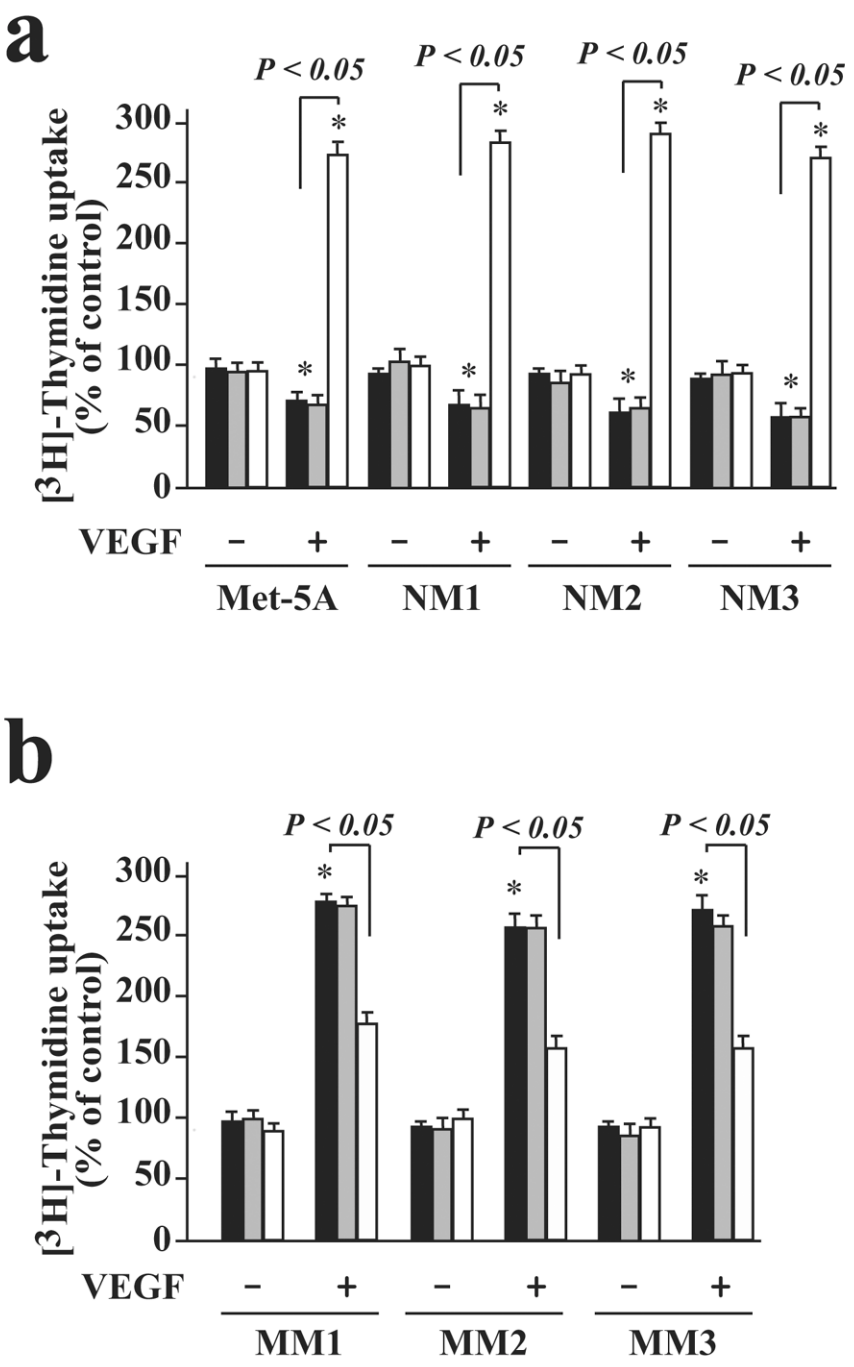

Figure 4. Role of p38 MAPK in VEGF-induced mesothelial cell proliferation. (***a***) Met-5A mesothelial cell line and three different primary normal mesothelial cells (NM1, NM2, NM3) were synchronized for 4 h in serum-free media. Cells were then incubated for 20 h in the absence or presence of 10 ng/mL VEGF. 10 μM of SB202190 (□), its analog SB202474 (■), or vehicle alone (■) was added to the culture medium 1 h prior to the mitogen. VEGF incubation was followed by the addition of 0.5 μCi of [^{3}H]thymidine for additional 4 h. Cells were next washed, lysed, and counted in a β-counter. (***b***) Malignant mesothelioma cells (MM1, MM2, MM3) were transiently cotransfected with 3 μg pcDNA3 plasmid coding MKK3 and 3 μg pcDNA3 expressing MKK6 (MKK3/6) (□), alternatively 6 μg empty vector (■), or with transfected mixture alone (Control) (■). After 24 h, cells were treated with 10 ng/mL VEGF for additional 24 h and [^{3}H]thymidine uptake was determined as described above. Data are the mean ± SD from 3 independent experiments, done in duplicate. *, $P < 0.05$ vs. control.

Fig. 5

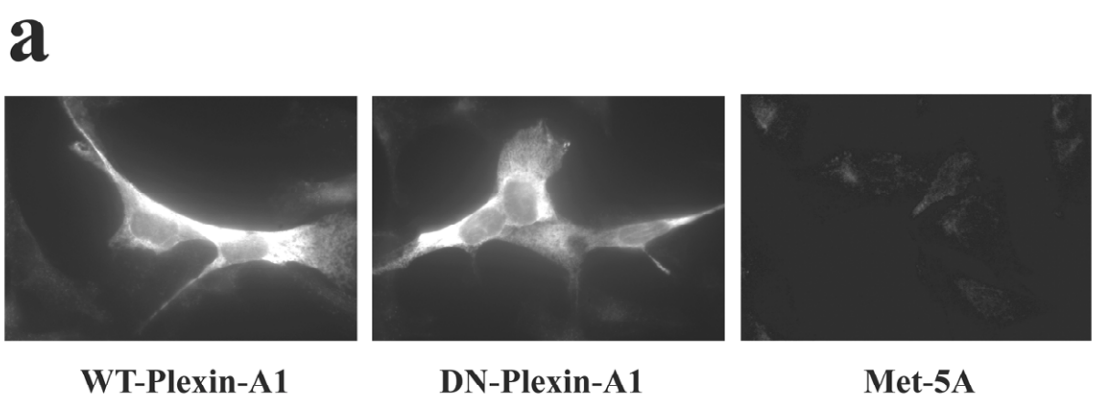

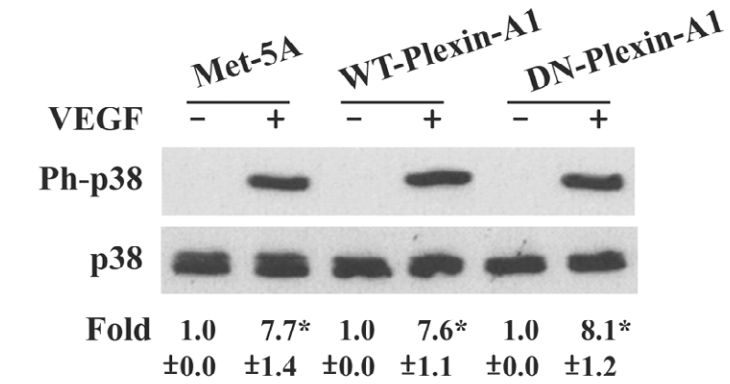

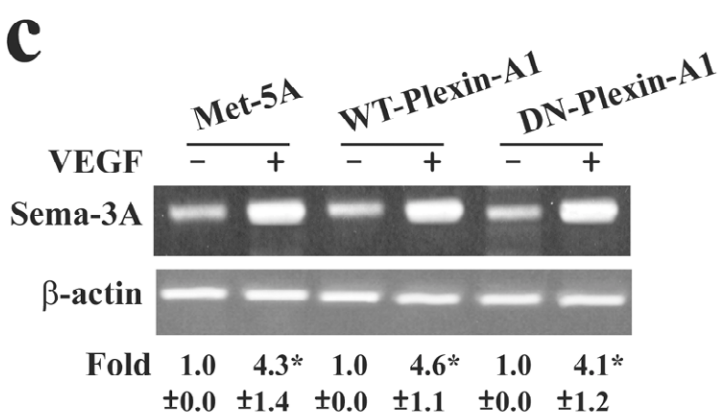

Figure 5. Plexin-A1-DN expression in Met5-A mesothelial cell line did not negate the stimulation of p38 MAPK signaling and Sema-3A up-regulation induced by VEGF. The mesothelial cell line, Met-5A, was engineered by lentiviral-mediated gene-transfer of GFP, plexin-A1 (WT-plexin-A1), or a truncated form of plexin-A1, lacking its cytoplasmic domain (DN-plexin-A1). (***a***) The infected cells were incubated for 3 min at 37°C in PBS^{2+}. The cells were fixed, and plexin proteins were localized by immunofluorescence, using antibodies directed against the VSV epitope tag included in plexin constructs. DN-plexin-A1, WT-plexin-A1, or parental Met-5A cells (2×10^5/mL) were exposed to the indicated concentrations of VEGF for the 48 h (***b*** and ***c***). (***b***) Phospho-p38 MAPK and total p38 MAPK were determined by Western blot as described in the legend to **Fig. 3*b***. (***c***) Sema-3A expression was determined by RT-PCR as described in the legend to **Fig. 2*a***. β-actin was used as internal control. Representative data from 3 independent experiments are shown (***b*** and ***c***).

Fig. 6

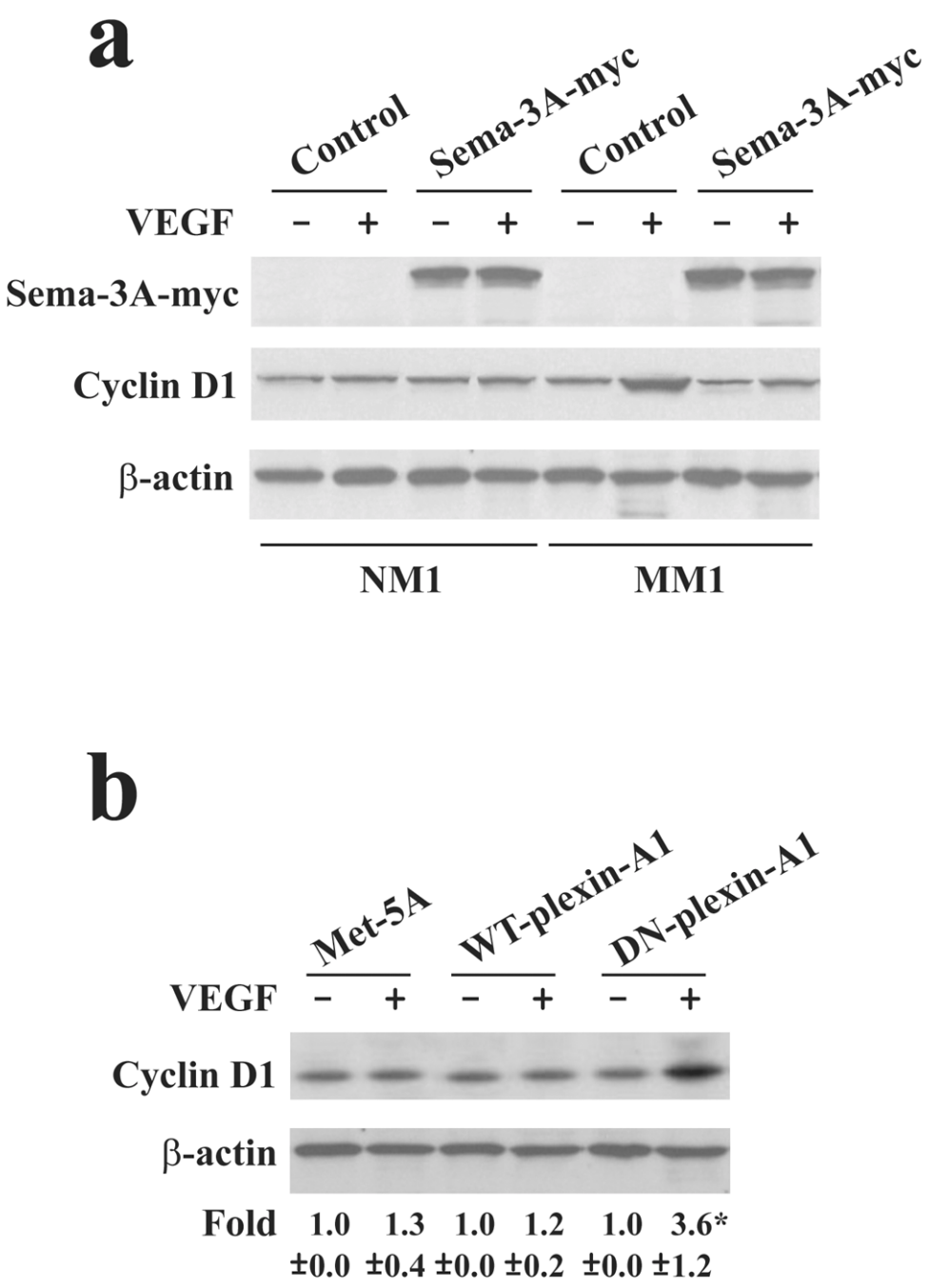

Figure 6. VEGF-stimulated cyclin D1 synthesis is inhibited by Sema-3A-dependent signals. (***a***) NM1 and MM1 cells were transiently transfected with 2 μg of either control vector (pcDNA3) or c-myc-tagged Sema-3A construct. After 24 h, cells were then incubated for an additional 24 h with or without 10 ng/mL of VEGF. Cell lysate protein was immunoblotted with anti-c-Myc (top) or anti-cyclin D1 (middle) antibody. β-actin served as loading controls. (***b***) Met-5A cell line, WT-plexin-A1 cells, and DN-plexin-A1 cells were treated for 24 h with VEGF (10 ng/mL). Cellular proteins were then extracted, and immunoblotted with anti-cyclin D1 antibody and normalized with respect to β-actin protein. Representative experiments (n=3) are shown (***a*** and ***b***). Folds are indicated as reported in **Fig. 2**. The relative ratio measured in the control without VEGF is arbitrarily presented as 1. Numbers represent the mean ± SD (n=3). *, $P < 0.05$ vs. control (***b***).